242 (2024) 213245

Contents lists available at ScienceDirect

Geoenergy Science and Engineering

journal homepage: www.sciencedirect.com/journal/geoenergy-science-and-engineering

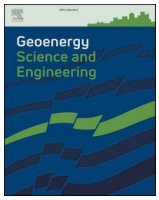

The effect of well temperature on the microstructure and the mechanical performance of bismuth-based plugs in well plugging and abandonment operations

Andriani Manataki [a,*], Lewaa Hmadeh [a], Bjørn Eske Sørensen [a], Paraskevas Kontis [b], Sigbjørn Sangesland [a]

[a] Department of Geoscience and Petroleum, Faculty of Engineering, Norwegian University of Science and Technology (NTNU), S. P. Andersens veg 15A, 7031, Trondheim, Norway
[b] Department of Materials Science and Engineering, Faculty of Natural Science, Norwegian University of Science and Technology (NTNU), 325 Kjemiblokk 1 Gløshaugen, 7034, Trondheim, Norway

ARTICLE INFO

Keywords:
Near-eutectic BiSn alloy
Plugging and abandonment
SEM/EBSD analysis
Tensile tests
Hydraulic push-out tests

ABSTRACT

Bismuth-tin (BiSn) alloys are considered promising candidates as potential alternatives to cement for well plugging and abandonment (P&A) applications to prevent any uncontrolled flow of deep reservoir fluids to the surface. As the temperature in the well varies with depth, the final microstructure of the BiSn alloy after its solidification might be influenced, and consequently the mechanical performance of the alloy will also be affected. The aim of this study is to evaluate the microstructural evolution of the BiSn alloy after solidification, at temperatures between 20 °C and 90 °C, to reflect in situ conditions from approximately 800m to 3 km depth. Microstructural characterization was carried out by using scanning electron microscopy (SEM) and electron backscatter diffraction (EBSD). The microstructural analysis revealed that the plug subjected to the lower temperature resulted in finer microstructure, whereas the grain size of the material was increased at higher temperatures. Additionally, the theoretical lever rule was employed to validate the microstructural findings. The observed microstructures were also correlated with tensile tests, which showed that the plug at 20 °C had a yield strength of 67,25 MPa, whereas the yield strength of the plug at 90 °C was only 41,64 MPa. In addition, hydraulic push-out tests further confirmed that lower testing temperatures correlate with higher pressure tolerance of the plug. The plug at 20 °C could withstand 113,5 bar, compared to the plugs at 60 °C and 90 °C which could withstand 90,4 and 50,9 bar, respectively. From all the experimental tests conducted, the outcome was that the lower temperature of 20 °C resulted in a material with a finer microstructure, which plays an important role in enhancing the mechanical properties of the bismuth-based plug. This study aims to advance the understanding of BiSn alloy performance in plug and abandonment (P&A) operations, thereby supporting the industry's efforts to qualify BiSn alloys as effective well-barrier materials.

1. Introduction

Well plugging and abandonment (P&A) is a necessary phase when a well reaches the end of its life. An essential aspect of P&A is to ensure well integrity after the abandonment (Vrålstad et al., 2019). The aim is to install a barrier material designed to avoid any leakage paths into the surrounding formations, which may end up contaminating the environment and all the directly affected organisms (Khalifeh and Saasen, 2020). Different types of well-barrier materials are used, but cement is the most common one. Nowadays most wells are still plugged with cement using methods and materials developed in the 1970s (Technology Subgroup of the Operations and Environment Task Group, 2011). Expandable cement for example is an improved form of cement with additives. However, there are still question marks regarding the

Abbreviations: BiSn, Bismuth-tin alloy; &A, Plugging and Abandonment; SEM, Scanning electron microscopy; EBSD, Electron backscatter diffraction; SCSSV, Surface Controlled Subsurface Valve; BSE, Backscatter electron; IPF, Inverse pole figure.

* Corresponding author.
E-mail addresses: andriani.manataki@ntnu.no (A. Manataki), lewaa.hmadeh@ntnu.no (L. Hmadeh), bjorn.sorensen@ntnu.no (B.E. Sørensen), paraskevas.kontis@ntnu.no (P. Kontis), sigbjorn.sangesland@ntnu.no (S. Sangesland).

https://doi.org/10.1016/j.geoen.2024.213245
Received 17 June 2024; Received in revised form 2 August 2024; Accepted 15 August 2024
Available online 22 August 2024
2949-8910/© 2024 The Authors. Published by Elsevier B.V. This is an open access article under the CC BY license (http://creativecommons.org/licenses/by/4.0/).

long-term integrity of cement in well construction and P&A operations. In particular, the cement may not withstand high temperatures, it may fail under high stress, and it may exhibit significant shrinkage over time and poor interfacial bonding (Barclay et al., 2001; Fulks and Carragher, 2020; Rios and Ars, 2021)

Thus, there is a great need for alternative materials, that can reduce the environmental impact of cement, while they allow for simple and robust plugging applications with reduced costs.

Recent studies have referred to some low melting point alloys, such as bismuth alloys, as a suggested alternative solution for well-barrier material (Khalifeh and Saasen, 2020; Vrålstad et al., 2019). Bismuth alloys are used for a wide range of applications, because of the range of their melting point, which is between 93 and 271 ^{o}C, depending on the alloying metal (Carragher P.J. & Fulks J., 2018; Zhang et al., 2019). This makes them also applicable for plugging applications in various formations. Bismuth plugs may also provide better isolation even with reduced plug lengths compared to cement plugs (Hmadeh, Jaculli, Elahifar, et al., 2024). Fig. 1 is a schematic sketch of a subsea well, indicating typical plug placement (Manataki et al., 2023; Sangesland et al., 2022). On the left side 3 cement plugs, each 50–100 m long, are installed at different depths, above the reservoir to prevent leakage of fluids into the environment.

Regarding the replacement of the cement with the BiSn (right well, Fig. 1), the aim is to plug the casings with a reduced plug length "X". Additionally, BiSn can fill the voids of the cracked cement, placed in the annulus between the casing strings, or between the casing and the surrounding formation.

The Bi based alloys take the property of bismuth to expand during solidification, making them candidates with good sealing capability between the alloy and the casing steel. So, in case of using bismuth-based plugs, two different conditions may arise in terms of the barrier quality of the cement behind the casing.

1) The expansion could positively reflect on the cement behind the casing, in case there were some cracks or empty voids/microannulus where they will be forced to be shut.
2) The expansion may negatively affect the integrity of the cement behind the casing, where this expansion could induce cracks in it. This part of the study is still under investigation, with not solid conclusions drawn yet (Hmadeh, Feneuil, Wiggen, et al., 2024).

The alloy used in the current study is the near-eutectic BiSn alloy which has a melting point of 139 °C. Consequently, it may not be suitable for applications at depths where the temperature can reach 90–100 °C. Therefore, for these higher temperature conditions, alternative metal alloys should be considered. For instance, a bismuth-based alloy with additions of other metals, to increase the melting temperature, could be a potential option. Additionally, alloys based on metals other than bismuth should also be evaluated for their suitability in higher-temperature applications.

Several studies (Hmadeh, Jaculli, Elahifar, et al., 2024; Hmadeh, Manataki, Jaculli, et al., 2024; Zhang et al., 2019) elaborate on the significance of bismuth as a key material alternative to cement and underscore the superior qualifications of bismuth-based alloys as well barrier materials compared to pure bismuth metal. However, there exist notable technological gaps and a scarcity of practical deployment experience concerning bismuth alloys. To ensure their proper and approved use, bismuth-based plugs must fulfill the requisite criteria outlined in NORSOKD-010 (2021) for certification as well-barrier materials (NORSOK standards, 2021). Key prerequisites include

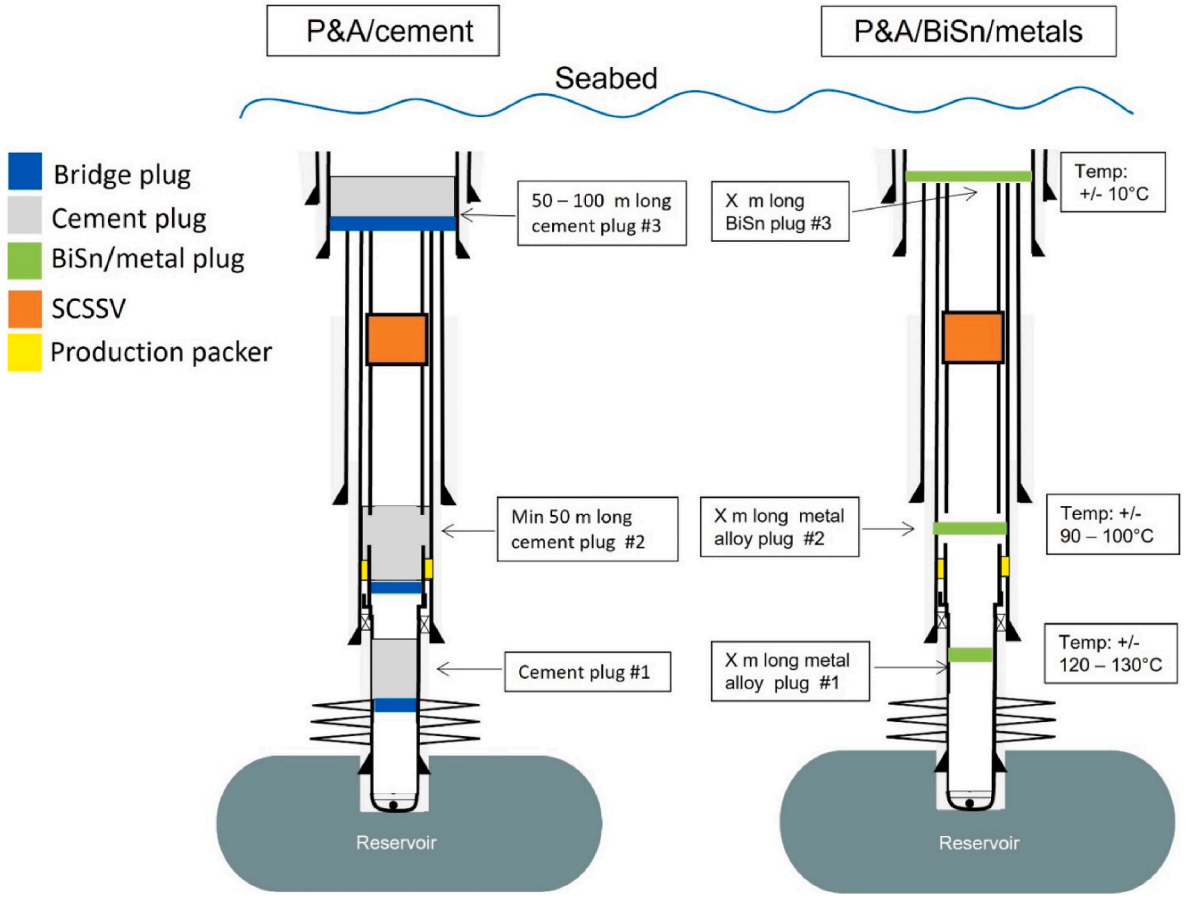

Fig. 1. Well plugging materials, cement vs. bismuth alloys and other metals. Note that X corresponds to the required length, depending on the properties under investigation (Sangesland2022), (Manataki et al., 2023).

demonstrating long-term integrity, impermeability, and resistance to mechanical loads. Therefore, additional research into the physical and mechanical characteristics of these plugs is imperative for engineers to comprehend their response to variations in parameters like temperature and pressure. Initial trials involving the utilization of bismuth-based plugs have been undertaken in the Valhall field, located in the southern region of the Norwegian North Sea (Thorstensen et al., 2022). More specifically the reference is to the eutectic BiSn alloy which has a low melting point of 135–139 °C (varies according to the manufacturer). In this study, a near eutectic alloy is used for experiments, to evaluate the impact of well temperature on both the microstructure and mechanical properties of the alloy. Specifically, testing is conducted at temperatures of 20 °C, 60 °C, and 90 °C. These temperatures correspond to various depths along the well.

2. Materials and methods

The near-eutectic BiSn alloy used in the current study is a product from the company 5N Plus (5N Plus, 2012). The alloy consists of 55 wt% Bi and 45 wt% Sn, and it has a melting temperature of 139 °C.

It is produced in the form of circular pellets, each one with a weight of 1 kg. The alloy is melted at 185 °C, using a heating furnace, provided by Binder company (Binder Company, 2024). Once melted, it is cast into the mold and allowed to air cool and solidify at ambient temperature as shown in Fig. 2. A steel pipe of S355 steel is used as a casting mold, with a height of 25 cm. The bottom 9.5 cm of the pipe was filled with casting sand, followed by a 12.5 cm layer for the cast BiSn alloy, while the remaining 3.4 cm were allocated to facilitate easier insertion of the plug into the setup for the subsequent mechanical tests (Fig. 3). In the present experimental investigation, six similar samples were prepared, with two samples allocated for each of the three designated testing temperatures: 20 °C, 60 °C, and 90 °C. Subsequently, each pair of samples was placed within a furnace concurrently linked to two pumps. The furnace was initially set to a temperature of 185 °C to ensure complete alloy remelting within the pipes under a pressure of 40 bar. The decision to use this pressure value was based on a previous study, which showed that the BiSn plug exhibits better sealing performance at 40 bar pressure compared to higher pressures (Hmadeh, Elahifar, Sangesland, et al., 2023). Once the alloy reached its molten state, typically after approximately 3 hours, the furnace temperature was adjusted to the specified testing temperature. The temperature was decreased at the same cooling rate for all the samples. The samples remained at these temperatures while simultaneously being subjected to the same pressure (40 bar) for 96 hours.

Upon completion of this period, one of the two pipes from each temperature group underwent material characterization via scanning electron microscopy (SEM) and electron backscattered diffraction (EBSD) analysis, as well as tensile testing, while the other pipe was utilized for hydraulic push-out testing.

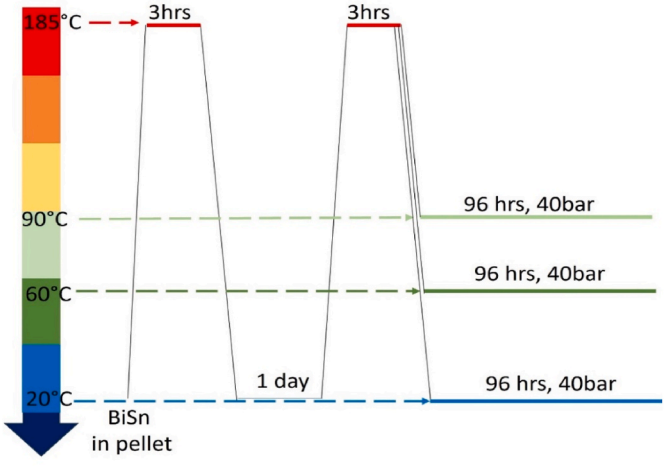

Fig. 2. Experimental procedure.

2.1. Microstructural characterization

After casting the BiSn alloy in the pipes, the samples were left at room temperature and atmospheric pressure. A 3 mm disk was then cut from the middle section of each sample as illustrated in Fig. 3 (Hmadeh, Manataki, Jaculli, et al., 2024). The disk was subsequently sectioned into four quarters, one of which was selected for preparation for microstructural characterization. The samples underwent mechanical grinding using abrasive media, SiC papers. To mitigate the risk of silicon carbide particles from the grinding paper embedding into the soft surfaces of both phases of the BiSn alloy, the samples underwent ultrasonic cleaning in alcohol after each grinding step. After grinding, two stages of polishing were conducted, initially using 3 μm diamond particles followed by 1 μm particles. Oxide polishing suspension (OP-S) was used for additional polishing. The samples were analyzed by SEM by using a Hitachi SU-6600 SEM, with an acceleration voltage of 20 kV. Images were collected in backscattered mode. EBSD data collection was conducted at the same conditions using the NORDIF camera and software. EBSD data were indexed using the EDAX OIM 7.2 software and indexed data were postprocessed using the MTEX toolbox (Bachmann et al., 2010 (Bachmann et al., 2011),) using the cleanup procedures outlined by Sørensen (Sørensen et al., 2020) and IPF colormaps of Nolze and Hielscher (Nolze and Hielscher, 2016) to avoid color jumps associated with minor orientation changes. EBSD maps were collected from various points along the length of the samples to provide detailed information regarding the grain size and the orientation of the grains within the BiSn alloy.

2.2. Tensile tests

Tensile tests were performed to collect information regarding the yield strength of the BiSn alloy that can be used for its qualification as well-barrier material.

This study aims to examine the behavior of BiSn plugs under varying temperatures, simulating conditions as closely resembling those found in oil and gas fields. Consequently, when a plug is positioned at a particular depth, it is subjected to a corresponding temperature. This does not apply only to the plug, but to the surroundings as well. Therefore, it is reasonable that the tensile tests conducted in this study were performed at temperatures matching those at which each sample was prepared, as explained earlier in section 2.

For this study, an MTS 880 testing machine (Skaret, 2014) was used, equipped with a 100 kN load cell and a 25 mm extensometer. The tests were conducted at a test speed of 9 mm/min at room temperature and at 90 °C. Tensile specimens with a gauge length of 30 mm, width 4 mm and thickness of 2 mm were wired-cut of the cast alloys (Fig. 4).

2.3. Hydraulic push-out test

Conducting push-out tests helps assess how well a material can withstand stresses resulting from thermal and mechanical loading in a well. The hydraulic push-out test is a straightforward laboratory experiment designed to measure the bond strength between materials, indicating the minimum pressure required to cause the bond to fail, leading to the material's detachment. Similar tests have been conducted with cement. Thermal and mechanical loading of the well, and deformation of surrounding rocks can damage the bulk of the cement sheath and its shrinkage over time may introduce a discontinuity, known as microannulus, between the casing and the cement (Lavrov et al., 2019). The microannulus may lead production fluids (gas, oil) to migrate to upper geological layers and contaminate the environment. Therefore, there must be a good bonding/adhesion, interaction, or connection

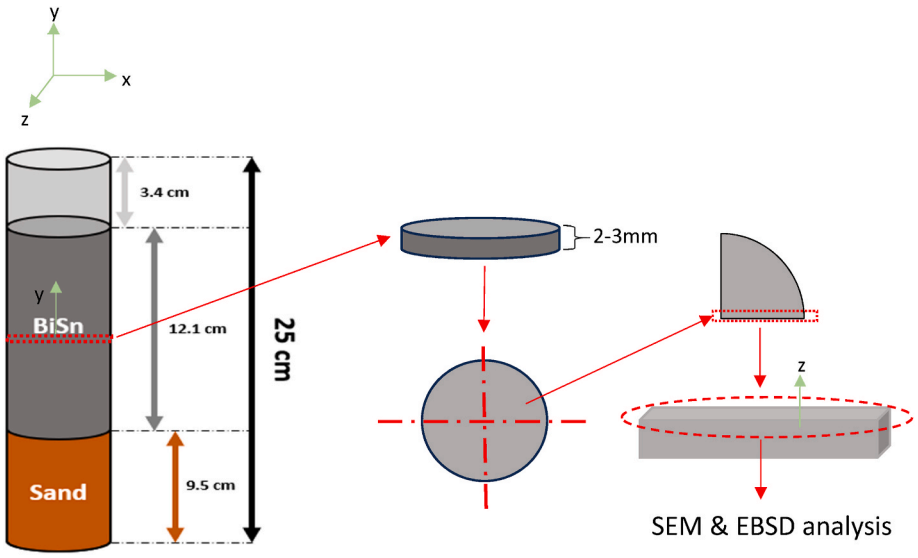

Fig. 3. Samples' preparation for microstructural characterization; 3 mm disk from the middle of the BiSn plug was taken and cut in 4 quarters.

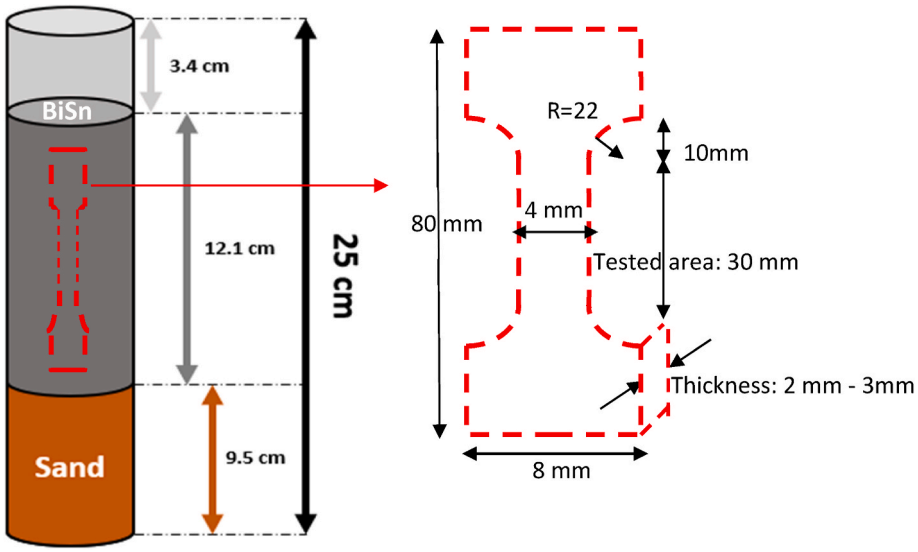

Fig. 4. Specimen preparation for tensile tests.

between the steel and the well barrier material, to prevent the creation of a microannulus.

The experimental procedure is outlined as follows: Initially, the BiSn alloy is cast into the pipe and allowed to solidify at ambient temperature. Subsequently, the solidified alloy-filled pipe is inserted into the test cell as shown in Fig. 5, which is then placed within the furnace. The furnace is set to 185 °C and maintained at this temperature for 3 h to facilitate the remelting of the plug, all while applying a pressure of 40 bar. Once the plug is completely melted, the temperature is adjusted to the desired level, with a constant pressure of 40 bar. This process is replicated three times, yielding three samples prepared under identical conditions, with varying setting temperatures of 20 °C, 60 °C, and 90 °C. Upon reaching the designated temperature, each sample was left under pressure (40 bar) for a period of 96 hours before the commencement of the hydraulic push-out tests.

For this study, the hydraulic push-out tests follow the same experimental procedure described in (Hmadeh, Elahifar and Sangesland, 2023). Water is used as the injection fluid to test this bond. During the test, water pressure is incrementally increased, at a predefined pumping rate of 0.4 ml/min, until the material's sealing capacity is exceeded, causing it to dislodge and slide. This movement results in a pressure decrease, signaling the failure of the hydraulic bond and the start of water leakage through newly formed microannuli at the plug-pipe interface. Once water is leaking at the bottom outlet of the test cell, the experiment ends.

The setup used for the push-out experiment is illustrated in Fig. 5. The pump will raise the pressure above the plug as it continuously pumps water at a predetermined rate. The plug will fail after its maximum sealing capability has been reached, and it will slide downwards. At the same time, a pressure drop will be observed, as the hydraulic bond fails, which reveals the opening of small gaps, through which water will pass towards the bottom outlet of the test cell, and start leaking, which indicates the end of the experiment.

3. Results and discussion

3.1. Microstructural characterization

Backscatter electron (BSE) images, EBSD phase maps, and inverse pole figures (IPF) are illustrated in Fig. 6. IPFs give a representation used

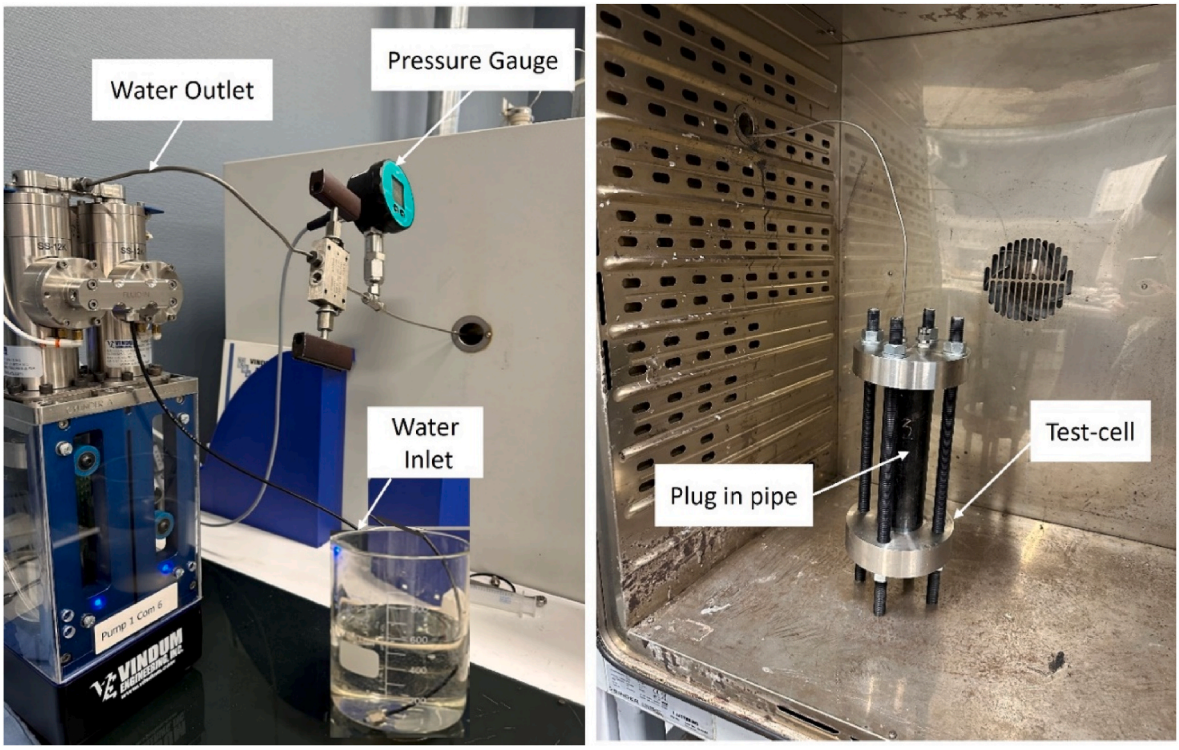

Fig. 5. Hydraulic pump connected to a test cell placed inside a heating cabinet.

to visualize the orientation of crystallographic grains within a material (Nolze and Hielscher, 2016). Each color in the IPF map corresponds to a specific crystallographic orientation (Kaushik et al., 2022). The distribution of colors in the IPF maps reveals the orientation of the grains. A more homogeneous distribution of orientations, is indicated by a more uniform color spread, as depicted in Fig. 6 g. A homogeneous microstructure is often preferable to ensure that stresses are homogeneously distributed during mechanical testing.

In Fig. 6 (a,b,c) the darker contrast indicates phases enriched with the lighter element, tin, identified as eutectic Sn, while the regions with the brighter contrast denote phases enriched with the heavier element, bismuth. At a temperature of 20 °C, the microstructure of the alloy resembles that of a eutectic structure (Fig. 6a). This can be more easily understood, comparing the phase maps Fig. 6 (d,e,f) where the grey color represents the tin and the red represents the bismuth. At elevated temperatures of 60 °C and 90 °C, Fig. 6(e and f) larger particles with dark contrast are observable along with smaller irregular white particles. The former correspond to primary Sn (α-Sn) phases, while the latter to Bi precipitates that have spherical or ellipsoidal morphologies (Manataki et al., 2023). Similar images for the BiSn microstructure have also been extracted in other studies (Božinović et al., 2021; Haubert et al., 1995; Mokhtari and Nishikawa, 2013; Silva et al., 2015). However, a microstructural investigation of the BiSn alloy, subjected to 40 bars and temperatures of 20 °C, 60 °C, and 90 °C for 96 h, has not been previously published.

The characterization of the alloy via SEM and EBSD analyses has revealed a notable trend: finer microstructures are observed at lower temperatures. There appears to be a correlation between temperature elevation and an increase in grain size. This phenomenon aligns with the principles outlined in solidification theory (Kurz and Fisher, 1998). More specifically, at lower temperatures, the molten alloy begins to solidify from numerous random nuclei simultaneously. These nuclei progressively grow until they intersect with neighboring grains, forming grain boundaries. Consequently, a fine-grained microstructure with abundant grain boundaries emerges. Such a microstructure is indicative of higher yield strength in the material as these boundaries impede the dislocations. As the temperature increases, the grain boundary density decreases, allowing in that way the atomic dislocations more easily. Higher temperatures provide atoms with greater thermal energy, causing them to vibrate more vigorously and move more rapidly within the material's crystal lattice. As a result, atoms are more likely to overcome energy barriers and migrate from one location to another. So, at higher temperatures, the increased thermal energy facilitates enhanced atomic diffusion, promoting the movement of atoms along grain boundaries. This redistribution process ultimately contributes to the coarsening of the material's microstructure.

The fluctuation in grain size can be reasonably attributed to the variations in each element at each temperature, as illustrated in Fig. 7. The most notable difference is observed for the primary Sn. At 90 ^{o}C, a coarser grain size of 21 μm is observed compared to 3 μm at 60 ^{o}C, which is much smaller, and no α-Sn is found at 20 ^{o}C. The presence of primary Sn contributes to the heterogeneity of the alloy at 60 ^{o}C and 90 ^{o}C Fig. 6 (b and c) comparing to the homogeneous microstructure observed at 20 ^{o}C in Fig. 6a.

Utilizing the lever rule allows for determining the elemental composition at each temperature. Understanding the lever rule is facilitated by referencing the phase diagram of the material. The application of the lever rule for the BiSn alloy is presented in Appendix A and the results are summarized in Table 1 which illustrates that with increasing temperature, the volume of Sn (Vα) increases, while the volume of Bi (Vβ) diminishes.

It is imperative to clarify that the measurement of Vα pertains to the combined volume of both primary Sn and eutectic Sn present in the microstructure. Using the "ImageJ" tool, phase fraction measurements can be done. The application of the ImageJ tool in this work was based on the step-by-step instructions provided by Hariharan V. S. (V S Hariharan, 2018). More specifically, measurements of the primary Sn were conducted at 3 points within each sample, yielding representative values as follows: 13% primary Sn at 60 ^{o}C and 18% primary Sn at 90 ^{o}C.

These numbers indicate a positive correlation between temperature elevation and characteristics of the alloy, as will be detailed subsequently. Through the subtraction of these measured values from the

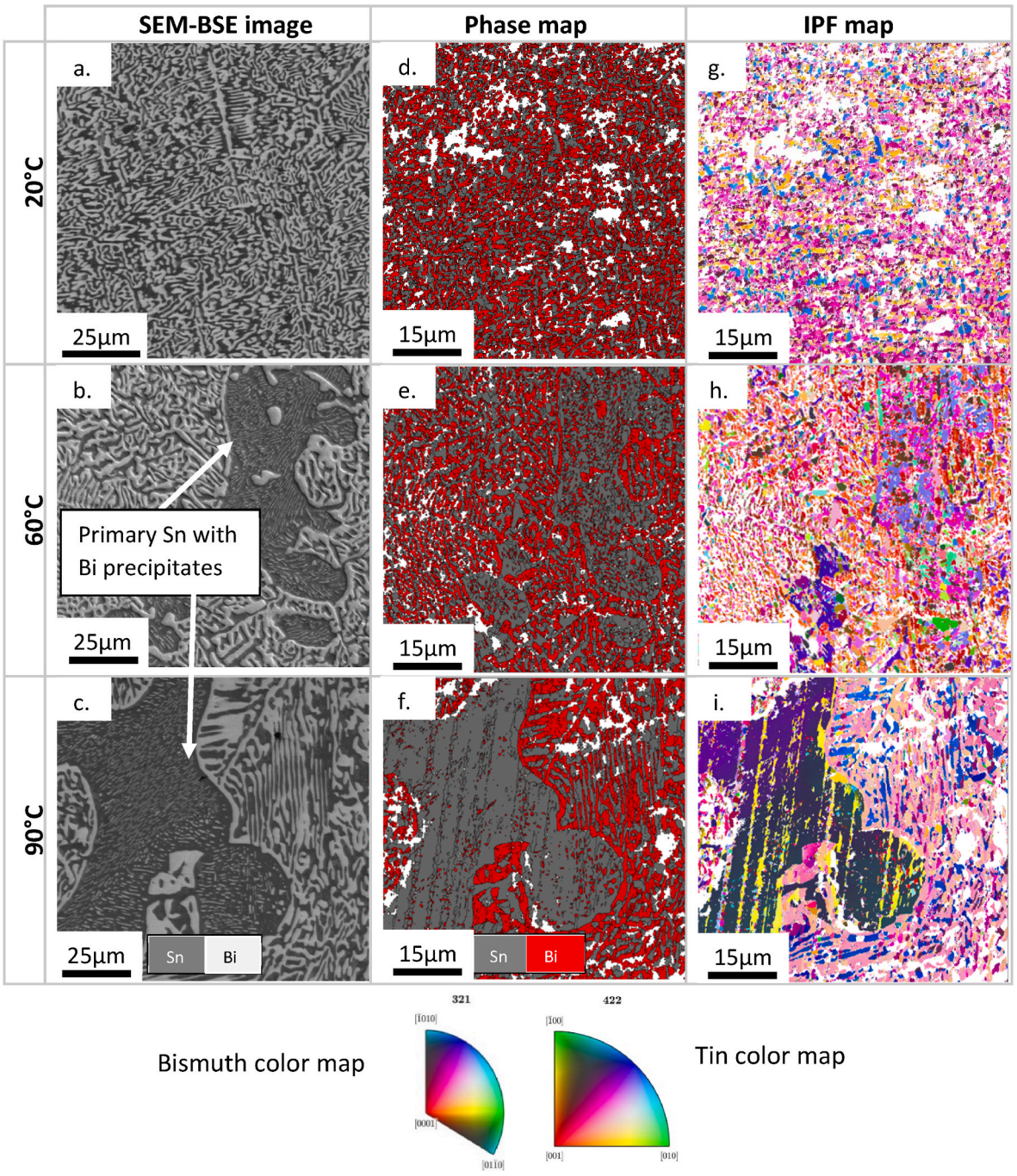

Fig. 6. SEM and EBSD images from identical points of the samples prepared at 20 °C, 60 °C and 90 °C.

total volume fraction of Sn delineated in the preceding table, we can determine the residual amount of Sn, thereby identifying the eutectic Sn composition, which accounts for 41 wt% and 38 wt% at temperatures of 60 °C and 90 °C, respectively.

3.2. Tensile tests

The engineering stress-strain curves in Fig. 8 demonstrate that the BiSn plug prepared at 20 °C exhibits a higher load-bearing capacity than the plug at 90 °C. Specifically, the yield strengths are measured at 67.25 MPa and 41.64 MPa, respectively. This observed discrepancy can be reasonably attributed to the microstructure of the BiSn plugs. The finer microstructure of the sample subjected to 20 °C (Fig. 6a) creates more grain boundaries, effectively impeding potential dislocations and resulting in a higher yield strength. It seems that the increased volume and grain size of primary Sn (Fig. 6b and c), which lead to inhomogeneous microstructures, also influence the mechanical properties of the BiSn plug.

Similar studies involving tensile tests on the BiSn alloy under the specific combination of 40 bars and temperatures of 20 °C, 60 °C, and 90 °C for 96 h does not appear to be extensively covered in the literature for comparison.

3.3. Hydraulic push-out test

Fig. 9 below displays the outcomes derived from the hydraulic push-out tests performed at each temperature, 20 °C, 60 °C and 90 °C, that each sample was subjected, as described in section 2.3.

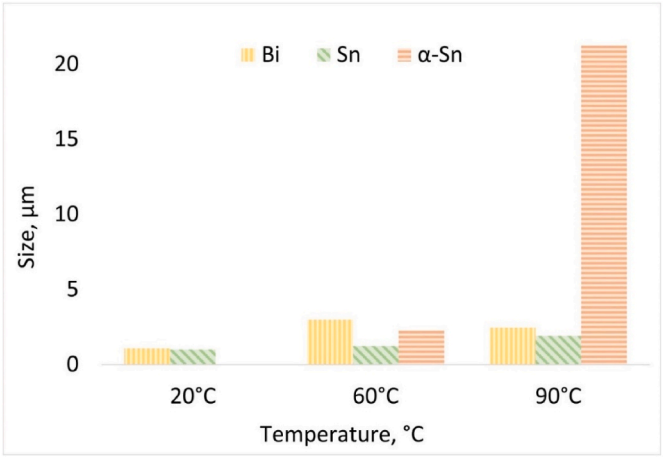

Fig. 7. Grain size of eutectic Bi, Sn and primary Sn (α-Sn).

Table 1
Mass fractions, volume fractions and densities of each phase in each temperature.

	20°C	60 °C	90 °C
Wα **%**	45	47	49
Wβ **%**	55	53	51
pα **(g/cm³)**	7.29	7.34	7.44
pβ **(g/cm³)**	9.75	9.75	9.75
Vα **%**	52	54	56
Vβ **%**	48	46	44

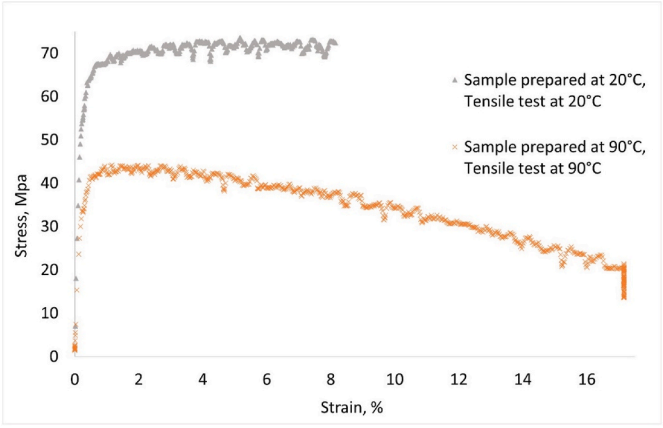

Fig. 8. Engineering stress–strain curve.

At 20 °C, the near-eutectic BiSn plug exhibited the highest recorded maximum pressure of 113.5 bar among the three tests conducted. Comparatively, the plug failed at 90,4 bar and 50,9 bar when tested at temperatures of 60 °C and 90 °C, respectively. Very similar values were obtained in a study investigating the effect of temperature on the hydraulic shear bond strength of the BiSn plug under comparable conditions (Hmadeh, Jaculli, Vedvik, et al., 2024). These results indicate a potential decrease in the shear bond strength of the bismuth plug with increasing temperatures. This observation aligns with the analysis derived from microstructural scans, indicating that finer microstructures contribute to enhanced plug stability by preventing dislocations. Consequently, the plug tested at 20 °C demonstrated prolonged durability and greater pressure resistance compared to the samples tested at higher temperatures. Once again, the substantial presence of primary Sn

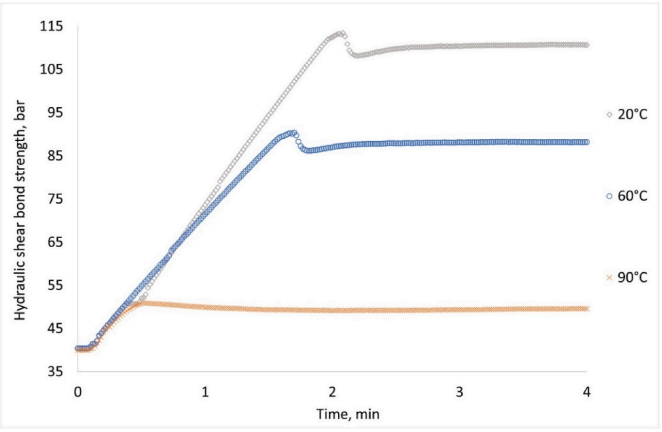

Fig. 9. Hydraulic push-out test.

grains notably influenced the material's behavior at each respective temperature.

It is important to highlight that the microstructure does not directly affect the shear bond strength of the material, but it affects the yield strength, which in turn has an impact on the shear bond strength. As depicted in Fig. 8, it was observed that at lower temperatures, the yield strength was higher. Thus, considering both results presented in Figs. 8 and 9, it is assumed that the sample with the higher yield strength will consequently possess a higher hydraulic shear bond strength.

4. Conclusions

In this work the resulting microstructure of the molten alloy during solidification at different well temperatures, 20, 60 and 90 °C was studied. From the microstructural analysis and the mechanical testing, the following conclusions can be drawn.

- at 20 °C the microstructure had finer grains and no α-Sn particles.
- the grain size was increased at higher temperatures. The volume of the primary Sn was increased with the increasing temperature as well. More specifically, 13% was observed in the sample subjected to 60 °C and 18% in the sample subjected to 90 °C.
- the presence of primary Sn with the increasing temperature increases also the heterogeneity of the microstructure of the alloy, reducing in this way its strength and integrity.
- the tensile tests indicated also that the plug at 20 °C could withstand a higher load, than the one at 90 °C. The yield strength for the first plug was 67,25 MPa, whereas, for the second plug, it was 41,64 MPa.
- regarding the hydraulic push-out tests, the conclusion was that lower testing temperatures correlate with higher pressure tolerance of the plug. It was observed that the plug at 20 °C could withstand 113,5 bar, compared to the plugs at 60 °C and 90 °C which could withstand 90,4 and 50,9 bar, respectively.
- all tests conducted with the sample at 90 °C yielded insufficient results, indicating that the material is unsuitable for use under these conditions in P&A applications.
- the key finding of this study is that the finer microstructure, achieved at 20 °C, plays a crucial role in enhancing the mechanical properties of the bismuth-based plug.

Overall, this study achieved its goal of better understanding the mechanical behavior of the BiSn alloy and how it is affected by the microstructure, which is influenced by the varying temperature parameter. This study can be a key contribution for the industrial qualification of bismuth as a well-barrier material.

However, further investigation on this topic is suggested. Additional experiments are needed to obtain more robust and reliable results.

Another avenue for investigation could involve replicating these experiments using a different BiSn composition, prioritizing the eutectic BiSn alloy with 58% Bi. Theoretically and in line with the lever rule, as employed in the current study, this alloy composition is expected to lack primary Sn within its microstructure, thereby influencing the mechanical properties of the material. Another valuable study would involve repeating the SEM and EBSD analyses on the samples after conducting the hydraulic push-out tests and tensile tests to examine how the microstructure is impacted. It would be interesting to investigate the fractured tensile specimens in order to understand the failure mechanism of this alloy. The long-term integrity of well barrier materials is crucial in P&A operations. Therefore, the long-term thermal exposure of BiSn plugs is currently under investigation by the same authors.

CRediT authorship contribution statement

Andriani Manataki: Writing – original draft, Methodology, Investigation. **Lewaa Hmadeh:** Writing – original draft, Investigation. **Bjørn Eske Sørensen:** Methodology, Investigation. **Paraskevas Kontis:** Writing – review & editing, Supervision. **Sigbjørn Sangesland:** Writing – review & editing, Supervision.

Declaration of competing interest

The authors declare the following financial interests/personal relationships which may be considered as potential competing interests: Andriani Manataki reports financial support was provided by Research Council of Norway. Lewaa Hmadeh reports financial support was provided by Research Council of Norway. If there are other authors, they declare that they have no known competing financial interests or personal relationships that could have appeared to influence the work reported in this paper.

Data availability

Data will be made available on request.

Acknowledgments

The authors acknowledge the Research Council of Norway (RCN) for financing the Center for Research-based Innovations "SWIPA - Center for Subsurface Well Integrity, Plugging and Abandonment", RCN project no. 309646, for which the work has been carried out. The center is also financed by the operating companies AkerBP, Equinor ASA, and Wintershall Dea Norway, and includes in addition more than 20 in-kind contributing industry partners. The R&D partners in SWIPA are SINTEF, NORCE, IFE, NTNU and UiS. Additional thanks must be given to Noralf Vedvik and Pål Christian Skaret, the laboratory technicians used to prepare the samples and the SEM analysis.

Appendix A

In Figure A. 1 (Alaskar et al., 2011) the lever rule is applied to the BiSn alloy with C0 = 55 wt% Bi (red line), at 90 °C (green line). The red line starts from the xx axis (mass % Bi) at the composition of Bi in the alloy which is equal to 55 wt%. and extends vertically upwards. A green line starts from the yy axis at the temperature studied, which in our case is 90 °C and is drawn parallel to the xx axis.

We assume that the phase α = Sn and the phase β = Bi. The composition of the α phase can be determined from the solvus line:

CBi(α) = concentration of Bi in the α phase = 9 wt%, and therefore.

CSn(α) = concentration of Sn in the α phase = 91 wt%,

The same procedure is then followed for the composition of the β phase:

CSn(β) = concentration of Sn in β phase = 0.1 wt%,

CBi(β) = concentration of Sn in β phase = 99.9 wt%.

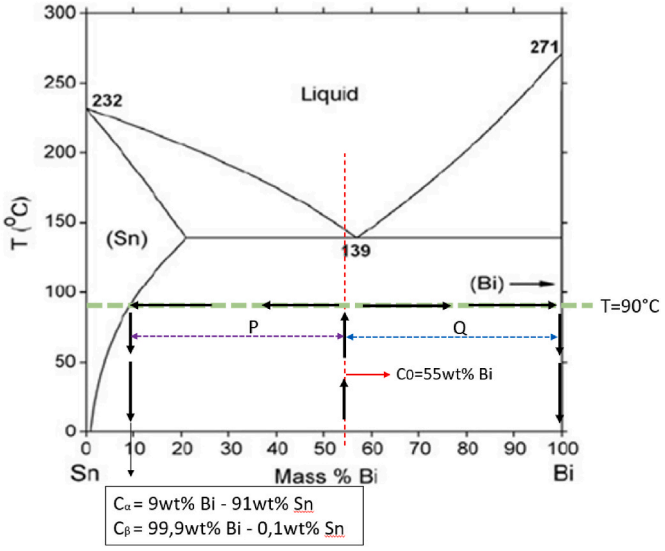

Fig. A. 1. Lever rule for the Sn55Bi alloy at 90 °C (the lever rule was applied on the phase diagram taken by (Alaskar et al., 2011).

The purple dashed line is the P corresponding to: C0- CBi(α)

The blue dashed line is the Q, which corresponds to: CBi(β) – C0.

The mass fraction of each phase can also be found using the following equations:

W_α = mass fraction of Sn,

W_β = mass fraction of Bi.

$$Wa = Q / (P + Q) = (\ CBi(\beta) - C0) / (\ CBi(\beta) - CBi(\alpha) = 49\% \quad (1)$$

$$W\beta = 1 - Wa = 0,51 = 51\% \quad (2)$$

The density of each element is pSn = 7.27 g/cm^3 and pBi = 9.75 g/cm^3. Since the concentrations of each component and their densities are known, the totaldensity of each phase, pα and pβ, can be calculated by using the equations below:

$$p\alpha = 100/(CSn(\alpha)/p_{Sn} + CBi(\alpha)/p_{Bi}) = 7.44\ \ g/cm^3 \quad (3)$$

$$p\beta = 100/((CSn(\beta))/p_{Sn} + (CBi(\beta))/p_{Bi}) = 9.75 g/cm^3 \quad (4)$$

Finally, now that we have the densities and the mass fractions of each phase, we can also find the volume of each component Vα and Vβ.

$$Va = (Wa / p\alpha) / (Wa / p\alpha + W\beta / p\beta) = 56\ \% \quad (5)$$

$$V\beta = 1 - V\alpha = 44\ \% \quad (6)$$

Accordingly, the same procedure is followed for the other two temperatures.

References

Alaskar, M., Ames, M., Liu, C., Connor, S., Horne, R., Li, K., Cui, Y., 2011. Smart nanosensors for in-situ temperature measurement in fractured geothermal reservoirs. In: Australian Geothermal Energy Conference. California. https://www.geothermal-energy.org/pdf/IGAstandard/AGEC/2011/GA20029.pdf.

Bachmann, F., Hielscher, R., Schaeben, H., 2010. Texture analysis with MTEX–free and open source software toolbox. Trans Tech Publications 160, 63–68. https://dx.doi.org/10.4028/www.scientific.net/SSP.160.63.

Bachmann, F., Hielscher, R., Schaeben, H., 2011. Grain detection from 2d and 3d EBSD data—specification of the MTEX algorithm. Ultramicroscopy 111 (12), 1720–1733.

Barclay, I., Pellenbarg, J., Tettero, F., Pfeiffer, J., Slater, H., Staal, T., Stiles, D., Tilling, G., Whitney, C., 2001. The Beginning of the End: A Review of Abandonment and Decommissioning Practices, vol. 13. Elsevier, pp. 28–41.

Binder Company, 2024. https://www.binder-world.com/int-en.

Božinović, K.N., Manasijević, D.M., Balanović, L.T., Gorgievski, M.D., Stamenković, U.S., Marković, M.S., Mladenović, Z.D., 2021. Study of microstructure, hardness and thermal properties of sn-bi alloys. Hem. Ind. 75 (4), 227–239. https://doi.org/10.2298/HEMIND210119021B.

Carragher, P.J., Fulks, J., 2018. Well abandonment solutions utilizing bismuth and thermite. Offshore Technology Conference. https://doi.org/10.4043/28897-MS.

Fulks, J., Carragher, P., 2020. Alternative abandonment material: bismuth. Day 2 wed, november 18, 2020, D023S008R003. https://doi.org/10.2118/202354-MS.

Hariharan, V.S., 2018. Phase fraction calculation of microstructure using ImageJ. https://doi.org/10.13140/RG.2.2.22990.51521.

Haubert, I., Dauphin, Y., Delplancke, J.-L., Charlier, J., Winand, R., 1995. Structural and dimensional stabilities of tin-bismuth fusible cores. J. Mater. Sci. 30, 4430.

Hmadeh, L., Elahifar, B., Sangesland, S., 2023a. The Sealing Behavior of Bismuth-Based Metal Plugs, vol. 9. Petroleum Technology, Offshore Geotechnics. https://doi.org/10.1115/OMAE2023-104309. V009T11A013.

Hmadeh, L., Elahifar, B., Sangesland, S., Abrahamsen, A.E., 2023b. A Full Laboratory Study on the Physical and Mechanical Properties of a Bismuth Plug. Day 3 Thu. https://doi.org/10.2118/212561-MS. March 09, 2023, D031S026R002.

Hmadeh, L., Feneuil, B., Wiggen, E., Skorpa, R., Sangesland, S., Elahifar, B., Anuncição Jaculli, M., 2024a. The effect of bismuth plug expansion on cement sheath integrity. Day 1 Wed. https://doi.org/10.2118/218458-MS. April 17, 2024, D011S005R002.

Hmadeh, L., Jaculli, M.A., Elahifar, B., Sangesland, S., 2024b. Development of bismuth-based solutions for well plugging and abandonment: a review. Petroleum Research 9 (2), 250–264. https://doi.org/10.1016/j.ptlrs.2024.01.003.

Hmadeh, L., Jaculli, M.A., Vedvik, N., Elahifar, B., Sangesland, S., 2024c. The effect of temperature on the sealability of bismuth–tin alloy plugs. Geoenergy Science and Engineering 241, 213107. https://doi.org/10.1016/j.geoen.2024.213107.

Hmadeh, L., Manataki, A., Jaculli, M.A., Elahifar, B., Sangesland, S., 2024d. A sealability study on bismuth-tin alloys for plugging and abandonment of wells. SPE J. 1–16. https://doi.org/10.2118/219744-PA.

Kaushik, L., Park, K.-S., Kim, J.-G., Lee, J.-S., Jeong, Y., Choi, S.-H., 2022. Reconstructing orientation data from the images of IPF maps and ODF sections extracted from the literature: a data-collection method for machine learning. Int. J. Plast. 159, 103467 https://doi.org/10.1016/j.ijplas.2022.103467.

Khalifeh, M., Saasen, A., 2020. Introduction to Permanent Plug and Abandonment of Wells, vol. 12. Springer International Publishing. https://doi.org/10.1007/978-3-030-39970-2.

Kurz, W., Fisher, D.J., 1998. Fundamentals of Solidification, 4th rev. Trans Tech Publications.

Lavrov, A., Bhuiyan, M., Stroisz, A., 2019. Push-out test: why bother? J. Petrol. Sci. Eng. 172, 297–302. https://doi.org/10.1016/j.petrol.2018.09.067.

Manataki, A., Kontis, P., Sangesland, S., 2023. Investigation of the microstructure of bismuth alloy and its interaction with cement and steel casing. Offshore Geotechnics; Petroleum Technology 9. https://doi.org/10.1115/OMAE2023-103843. V009T11A012.

Mokhtari, O., Nishikawa, H., 2013. Coarsening of Bi phase and intermetallic layer thickness in Sn-58Bi-X (X=In and Ni) solder joint. Proceedings - 2013 14th International Conference on Electronic Packaging Technology. ICEPT 2013, pp. 250–253. https://doi.org/10.1109/ICEPT.2013.6756465.

N Plus. https://www.5nplus.com/media/uploads/products/product/product_sheet/balloy_137_tech_data_sheet_2016-07-22-15-34.pdf, 2012.

Nolze, G., Hielscher, R., 2016. Orientations – perfectly colored. J. Appl. Crystallogr. 49 (5), 1786–1802. https://doi.org/10.1107/S1600576716012942.

NORSOK standards, 2021. Well integrity in drilling and well operations, NORSOK standards (version 1) [NAT]. https://online.standard.no/nb/norsok-d-010-2021ac2-2021.

Rios, R., Ars, F., 2021. Plug and abandonment materials—technology landscape. Day 4 Thu, August 19, 2021, D041S051R007. https://doi.org/10.4043/30938-MS.

Sangesland, S., Opedal, N., Vedvik, N., Manataki, A., Hmadeh, L., 2022. Bismuth based barrier materials – initial Results from 3rd party testing in SWIPA [Conference presentation]. 10th Norwegian Plug & Abandonment Seminar, Stavanger, Norway. https://www.offshorenorge.no/contentassets/398967cc39ee447b808f005e023ef1a2/bismuth-based-barrier-materials—initial-results-from-3rd-party-testing-in-swipa.pdf.

Silva, B.L., Reinhart, G., Nguyen-Thi, H., Mangelinck-Noël, N., Garcia, A., Spinelli, J.E., 2015. Microstructural development and mechanical properties of a near-eutectic directionally solidified Sn-Bi solder alloy. Mater. Char. 107, 43–53. https://doi.org/10.1016/j.matchar.2015.06.026.

Skaret, P.C., 2014. Mts 880. https://www.ntnu.no/wiki/display/imtlab/MTS+880.

Sørensen, B.E., Hjelen, J., Ånes, H.W., Breivik, T., 2020. Recent features in EBSD, including new trapezoidal correction for multi-mapping. IOP Conf. Ser. Mater. Sci. Eng. 891 (1), 012021 https://doi.org/10.1088/1757-899X/891/1/012021.

Technology Subgroup of the Operations and Environment Task Group, 2011. Plugging and Abandonment of Oil and Gas Wells (Paper #2-25, P. 21) [Working Document of the NPC North American Resource Development Study]. Operations & Environment Task Group. https://www.npc.org/Prudent_Development-Topic_Papers/2-25_Well_Plugging_and_Abandonment_Paper.pdf.

Thorstensen, E., Vadset, K., Straume, M.K., Delabroy, L., Abdelal, G., Carragher, P., Fulks, J., Mason, D.L., 2022. Bismuth plugs used to cap all wells during the final phase of the Valhall DP abandonment campaign, offshore Norway. Offshore Technology Conference. https://doi.org/10.4043/31897-MS. Houston, Texas.

Vrålstad, T., Saasen, A., Fjær, E., Øia, T., Ytrehus, J.D., Khalifeh, M., 2019. Plug & abandonment of offshore wells: ensuring long-term well integrity and cost-efficiency. J. Petrol. Sci. Eng. 173, 478–491. https://doi.org/10.1016/j.petrol.2018.10.049.

Zhang, H., Ramakrishnan, T.S., Elias, Q.K., Perez, A.J., 2019. Evaluation of bismuth-tin alloy for well plug and abandonment. SPE Prod. Oper. 35, 111–124. https://doi.org/10.2118/199363-PA.